Ion-beam-assisted hexagonal diamond formation from C_{60} fullerene

2003 J. Phys.: Condens. Matter 15 2899

(http://iopscience.iop.org/0953-8984/15/17/337)

INSTITUTE OF PHYSICS PUBLISHING JOURNAL OF PHYSICS: CONDENSED MATTER

J. Phys.: Condens. Matter **15** (2003) 2899–2906 PII: S0953-8984(03)54600-8

Ion-beam-assisted hexagonal diamond formation from C_{60} fullerene

X D Zhu[1,2], Y H Xu[1], H Naramoto[1], K Narumi[1], A Miyashita[3] and K Miyashita[4]

[1] Advanced Science Research Centre, JAERI, 1233 Watanuki, Takasaki, Gunma 370-1292, Japan
[2] Department of Modern Physics, University of Science and Technology of China, Hefei, Anhui 230026, People's Republic of China
[3] Department of Materials Development, JAERI, 1233 Watanuki, Takasaki, Gunma 370-1292, Japan
[4] Gunma Prefecture Industrial Technology Research Laboratory, 190 Toriba Maebashi Gunma 371-0845, Japan

Received 10 October 2002, in final form 14 February 2003
Published 22 April 2003
Online at stacks.iop.org/JPhysCM/15/2899

Abstract

Ions are commonly believed to be detrimental to diamond growth because of the high degree of lattice disorder induced by ion bombardments. In this paper, we examine the possibility of preparing diamond using thermally evaporated C_{60} and simultaneous bombardment with Ne^+ ions. It is found that the diamonds can be grown on Si wafers in the appropriate substrate temperature and ion energy ranges. Micro-Raman spectroscopy, x-ray diffractometry, and scanning electronic microscopy were employed to characterize the deposited specimen. These measurements provide definite evidence of the structure of nanosized hexagonal diamond. The mechanism responsible for the diamond formation is discussed.

Even though diamond growth by chemical vapour deposition has seen great success technologically and is well understood theoretically now, it is still a difficult challenge to prepare diamond under physical vapour deposition (PVD) conditions. Only recently has it been reported that growth of diamond on sapphire (0001) wafer has been achieved by pulsed laser deposition [1], in which oxygen etching of carbon is considered to be one mechanism important for diamond formation. Meanwhile, great efforts have been made to form diamond on the basis of ion beam techniques in the last decade. Unfortunately, the products are amorphous carbon films with a high fraction of sp^3 bonding [2]. Common wisdom has it that ions are detrimental to diamond growth, because collision cascades produce a high degree of lattice disorder.

Is ion bombardment always harmful to diamond growth, and can diamond be deposited under ion beam conditions? The answers to these questions are indeed intriguing; they would advance our fundamental understanding of the ion–diamond reaction.

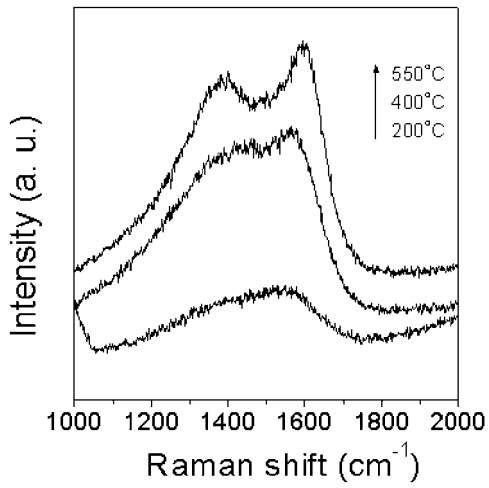

Figure 1. Raman spectra of the samples deposited under 1.5 keV Ne^+ ion bombardment at 200, 400, and 550 °C.

In the present study, we have examined the possibility of diamond formation under ion beam conditions. The deposition has been carried out using thermally evaporated C_{60} fullerene and simultaneous bombardment with Ne^+ ions. The reason for choosing C_{60} as the carbon source lies in its high chemical reactivity and unique bonding structure. C_{60}, a new form of solid carbon with the 'magic' cage molecular structure, consists of twenty hexagons involving sp^2 hybridization and twelve pentagons associated with sp^3 hybridization [3]. This novel feature makes it possible to take advantage of C_{60} to produce new functional material. It was reported that C_{60} fullerene has been squeezed into diamond under high pressure [4]. C_{60} ion impact is an important approach for transferring C_{60} to other forms of carbon. In the deposition, Ne^+ ions first bombard the C_{60} molecules to produce energetic carbon-containing species. These species can condense on the substrate to form films. On the other hand, Ne^+ ions also concurrently irradiate the growing films, which influences the chemical bonding structures. By choosing the preparation parameters to stimulate ion-induced surface dynamic processes favourable to diamond formation, we have successfully prepared diamonds on silicon (111) substrates.

Ion-beam-assisted deposition (IBAD) was used in this study. The machine was equipped with an ion gun and a Knudsen cell. The ion beam incidence angle was 60° from the substrate normal. C_{60} powder with a purity of 99.99% was placed in pyrolytic BN in the sublimator. The background pressure in the chamber was less than 1.2×10^{-6} Pa. The substrate temperature can be controlled from room temperature to 800 °C via resistive heating. Mirror-polished Si(111) wafers were used as substrates. C_{60} vapour was produced by resistively heating the Knudsen cell up to 400 °C, and simultaneously the growing film was bombarded with Ne^+ ions. The working pressure was maintained at around 6×10^{-4} Pa in the chamber. After the deposition, the bonding nature was analysed with a Renishaw 2000 imaging microscope using a 514 nm Ar^+ ion laser with a power less than 1 mW. For the structural analysis, an x-ray system (Geiger Flex RAD-III, RIGAKU) equipped with a powder diffraction goniometer was operated at 50 kV, 30 mA. The surface features of the sample were examined by scanning electronic microscopy (SEM).

We have carried out a series of experiments to investigate the dependences of the properties and structures of the deposited films on the substrate temperature under 1.5 keV Ne^+ ion

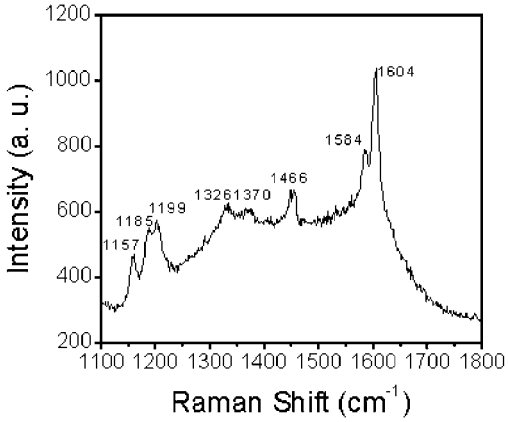

Figure 2. The Raman spectrum of the sample prepared at 700 °C substrate temperature and with 1.5 keV Ne^+ ion bombardment.

bombardment. Figure 1 depicts Raman spectra of the amorphous carbon films deposited at 200, 400, and 550 °C. Graphite has two significant Raman lines, the so-called G peak and D peak. The Raman spectrum at 200 °C presents a strong broad band centred at about 1537 cm^{-1}, indicating the structure of amorphous carbon. With substrate temperature increasing to 400 °C, however, slight separation of the G and D lines occurs. For amorphous carbon, the D and G lines tend to be separated; distinct peaks are indicative of more graphitic material. This phenomenon becomes more pronounced as the substrate temperature becomes higher than 400 °C.

At the growth temperature of 700 °C, the interesting finding is that several distinct Raman lines are observed for the centre region of the film, as shown in figure 2. There is a high ratio of Ne^+ ions to thermal C_{60} flux at the centre region of substrate, because the Ne^+ ion beam spot did not scan, in order to assist with producing a higher Ne^+ ion current. The first question is whether these Raman peaks originate from C_{60} or not.

In our previous work, we have investigated the influence of Ne^+ ion energy on the bonding structures at room temperature [5]. We found that C_{60} film can be prepared for Ne^+ ion energy up to 500 eV. The conversion from C_{60} structure to amorphous carbon takes place on increasing the Ne^+ ion energies to 700 eV; no significant Raman lines for C_{60} can be observed except for the D peak and G peak. In this case, under 1.5 keV ion bombardments, the Ne^+ ions possess high enough energies to convert C_{60} to amorphous carbon phases; figure 1 clearly shows the distinct amorphous carbon structures. On the other hand, it should be noted that C_{60} starts to evaporate at around 400 °C or lower temperatures. Considering the growth temperature and the Ne^+ ion energy dependence of the bonding characteristics for the deposited films, we believe that there is no C_{60} in the deposited films under 1.5 keV Ne^+ ion bombardment, especially at such high temperatures.

A wealth of Raman peaks are present in figure 2. Cubic diamond, a common product in chemical vapour deposition, is characterized by fourfold-coordinated sp^3 bonding of O_h symmetry; its first-order Raman mode is at 1332 cm^{-1}. The 1332 cm^{-1} mode of diamond is essentially the highest-energy vibrational mode of this structure, as is well determined theoretically and experimentally. In a study of the direct conversion of graphite into diamond, Bundy and Kasper [6] were the first to find a new phase that was identified as hexagonal diamond in addition to the conventional cubic diamond. Yagi *et al* [7] confirmed the pressure-induced phase transformation from graphite to hexagonal diamond at room temperature. The physical properties of cubic and hexagonal diamond are quite similar; the C–C atom bonding

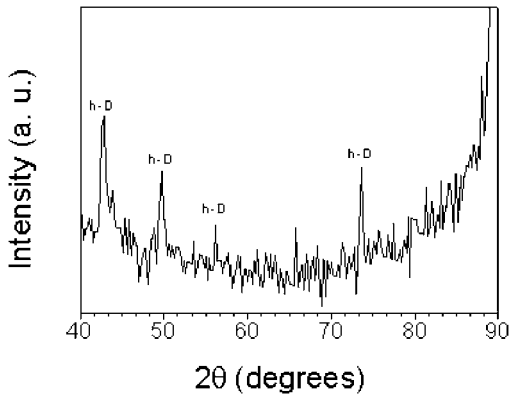

Figure 3. The XRD pattern of the film shown in figure 1. 'h-D' stands for hexagonal diamond.

for both structures is sp^3 bonding. The major difference between hexagonal diamond and cubic diamond comes from the stacking sequence of the identical puckered carbon layers. Cubic diamond is constructed with the stacking sequence 'ABCABC...', while hexagonal diamond has the 'ABAB...' stacking sequence [8]. The Raman spectrum of hexagonal diamond is distinct from that of cubic diamond. One can observe a slight shift of the first Raman line for cubic diamond from 1332 down to 1326 cm^{-1} in figure 2. This has been confirmed experimentally to be one Raman mode of hexagonal diamond, just below that of cubic diamond [9]. For hexagonal diamond, three Raman-active modes are predicted: A_{1g}, E_{1g}, and E_{2g}. According to the recent calculation by Wu *et al* [8], these three Raman-active modes are A_{1g} (1312 cm^{-1}), E_{1g} (1305 cm^{-1}), and E_{2g} (1193 cm^{-1}), respectively. The strong Raman line centred at 1199 cm^{-1} and the weak line at 1185 cm^{-1} in figure 2 are in fairly good agreement with the calculated E_{2g} Raman mode of hexagonal diamond, which is convincing evidence for hexagonal diamond. The broad features of Raman lines here might be correlated with the nanosize of the crystallites.

In diamond synthesis by a hydrogen plasma jet, Maruyama [10] obtained a mixture of many kinds of the hexagonal diamond polytype; the Raman band given is located at 1140 cm^{-1}. Likewise, the Raman peaks near 1150 and 1133 cm^{-1} have been assigned to the presence of the nanocrystalline phase of diamond in much of the literature [11, 12]. In our case, we observed a weak peak at 1157 cm^{-1}, which is similar to those findings. For ion-beam-based techniques, only a few reports have claimed to achieve diamond deposition. Unfortunately, in those reports, the evidence provided is from x-ray photoelectron spectroscopy [13] or the Raman spectra given have no significant Raman characteristic correlated with diamond except for the two sharp peaks, the D peak and G peak [14]. To the best of our knowledge, the evidence shown in this work is the first report of a distinct Raman feature for a diamond phase prepared by ion beam methods. Graphite has two significant Raman lines, the so-called G peak and D peak. The G peak around 1580 cm^{-1} is due to the Raman-allowed E_{2g} mode of crystalline graphite, and the D peak around 1350 cm^{-1} is associated with the disorder-allowed zone-edge mode of graphite. None of the features in the Raman spectrum with energy higher than 1332 cm^{-1} can be attributed to diamond structures with long-range order. In the region of high Raman shifts shown in figure 2, there appear big Raman shifts at 1370 and 1466, 1584 and 1604 cm^{-1}, which are assigned to disordered carbon and graphite, respectively.

Figure 3 shows the XRD pattern of the sample as analysed by micro-Raman spectroscopy. One can find several diffraction lines with various intensities. The calculated interplanar

Table 1. Measured interplanar spacings (d) of the sample; these values are compared with those expected for diamond and graphite from the Powder Diffraction File.

Sample	Cubic	2H-lonsdaletic	8H-hexagonal	12H-hexagonal	20H-hexagonal	Graphite
2.1130		2.19	2.11	2.15	2.14	2.14
	2.06	2.06	2.06	2.06	2.06	2.08
					1.93	2.03
1.8312		1.92	1.93	1.93	1.83	1.96
	1.79					1.81
1.6369			1.71	1.64	1.63	1.68
						1.55
1.4194		1.50				1.46
1.2871	1.26	1.26	1.26	1.26	1.26	1.23
						1.16
1.1099		1.17				1.11

spacings (d) based on this diffraction pattern are presented in table 1, where these values are compared with those expected from diamond and graphite, from the Powder Diffraction File. The interplanar spacings of the four strong lines are in rather good agreement with the values for 20H-hexagonal diamond. The corresponding peaks are indicated as h-D in figure 3. However, the origins of the remaining two diffraction lines are difficult to determine in this work; it is likely that they are originating from some impurities in the chamber or graphite. The size of the hexagonal diamond is estimated as of the order of 30 nm, based on the x-ray diffraction line. The x-ray measurement mainly manifests the features of 20H-hexagonal diamond. We believe that it gives further and consistent evidence for the structure of hexagonal diamond deduced from the Raman spectrum.

A SEM micrograph of the sample is shown in figure 4. No habit plane can be found in the SEM image, which agrees with the Raman and XRD analysis in indicating that the film consists mainly of the nanocrystallite polytype.

According the above analysis, hexagonal diamonds can form in appropriate conditions in this work. This observation is ascribed to the unique advantage of IBAD possesses. It is stated that IBAD involves not only a vapour process resulting from collisions between incident ions and molecules/atoms but also ion implantation. It is very possible that more than one mechanism takes effect in the diamond formation.

Two facts regarding IBAD should be noted. One concerns the ion–C_{60} reactions. Ne^+ ions ejected from the ion gun first react with C_{60} molecules in a vapour environment. In collisions, impact energy may be transferred to the internal energy of the clusters. When C_{60} possesses enough internal energy, the dissociation of C_{60} clusters may be induced. The actual mechanism of fragmentation is not completely clear as yet. A sequential C_2 loss mechanism has been proposed by a number of authors [15–17]. Also, *in situ* optical emission measurement reveals a strong green colour emission (Swan band) at 516.5 nm from the C_2 radicals in the C_{60} + Ar microwave plasma. The C_2 dimer is suggested to be responsible for the diamond growth [18–20]. In our case, it is reasonable to assume that the following dynamic processes take place: $Ne^+ + C_{60} \rightarrow Ne + C_{60}^+$, $C_{60}^+ \rightarrow C_{60-2n}^+ + nC_2$.

Since the energy transfer depends on the incident ion energy, ion-to-atom ratio, ion mass, target atom mass, and scattering angle, a lot of C_2 dimers with a wide energy range are generated as collision products. C_2 has been accepted as the growth precursor species for the formation of nanocrystalline diamond in both hydrogen-free deposition [18] and hydrogen-containing systems [20]. At the same time, carbon clusters possessing relatively high energy penetrate

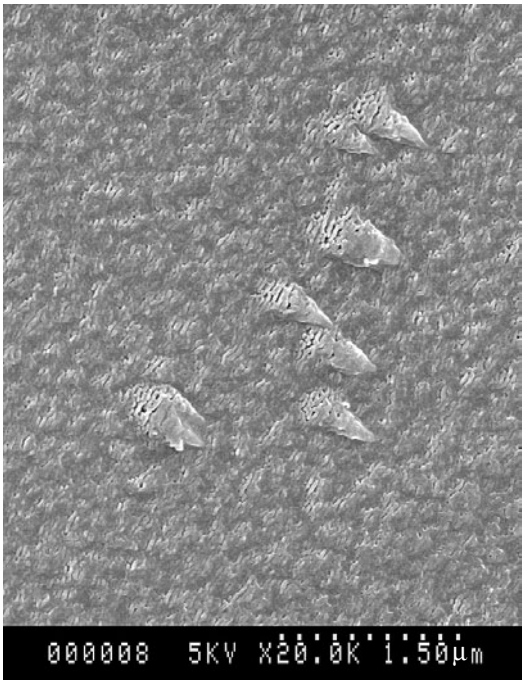

Figure 4. A SEM image of the sample.

into the subsurface of the growing film and serve as nucleation sites. Continuous addition of clusters must lead to high renucleation rates. This provides an important prerequisite for nanosized diamond formation. Likewise, the substrate is an important factor affecting diamond formation. It is believed that a high substrate temperature is generally required for diamond formation, even in chemical vapour deposition. Therefore, there exists a favourable growth condition for nano-diamond, which should be attributed to the presence of the nanocrystalline phase of diamond.

On the other hand, another fact should not be ignored during deposition: energetic species bombard the substrate. The total energy of hexagonal diamond is slightly higher than that of cubic diamond, which makes hexagonal diamond slightly less stable than cubic diamond. Since the environmental condition favourable to hexagonal diamond formation needs high carbon supersaturation, as in shock high-pressure methods, we may consider an analogue of shock quench in the ion–solid reaction—that is, a thermal spike. This term refers to localized melting produced by the bombardment of energetic species during film deposition. The portion of the energy transmitted to the lattice by incident ions can appear in the form of lattice vibrations concentrated locally, so the temperature could be sufficiently high on an atomic scale. For the thermal spike in the formation of tetrahedral amorphous carbon where the ions have an energy between 40–400 eV, the temperature can reach 5000 K, and the thermal spike cools in less than a picosecond [21]. Thus, the thermal spikes from ion collisions can provide conditions of high temperature and high pressure, but they rapidly collapse. This process resembles that of the shock quench method. We believe that hexagonal diamond formation can be ascribed to this kind of thermal-spike-induced atomic rearrangement in our case.

However, even if the phase change takes place, these diamond configurations hardly grow in the films, because they are surrounded by amorphous carbon, and also diamond may convert

to sp^2-bonding carbon at relatively high temperature. Therefore, if diamond can accumulate in the film, a competitive mechanism suppressing the graphite phase must exist simultaneously during deposition.

During deposition, the simultaneous irradiation of Ne^+ ions on the growing films will give rise to the asymmetric displacement of sp^2/sp^3 carbon atoms [22, 23]. There is a large difference in cross-section between irradiation-induced displacements of carbon atoms bound on sp^2 sites and on sp^3 sites under irradiation. Diamond has higher effective displacement threshold energies than graphite. This asymmetry leads to preferential damage of graphite. The unbalanced displacement of carbon atoms with sp^2 or sp^3 bonding gives rise to the accumulation of diamond. However, the preferential damage of graphite does not always take place under irradiation—which depends strongly on the substrate temperature. Only in an intermediate temperature regime do these interface interstitials recombine preferentially to diamond, with graphitization suppressed [22, 23]. Otherwise, graphite again becomes the stable phase. Our experiment clearly demonstrates the temperature dependence of diamond formation; a substrate temperature as high as 700 °C is absolutely essential for forming hexagonal diamond. From the above, one can note that diamond deposition by ion beam methods has a stricter growth parameter window.

In conclusion, the IBAD technique was employed to synthesize diamond. Nanosized hexagonal diamond was prepared using thermally evaporated C_{60} and a simultaneous Ne^+ ion bombardment of 1.5 keV at the substrate temperature of 700 °C. The measured Raman features for the deposited specimen are in good agreement with Raman modes predicted by theoretical calculations and observed in experiments, consistently with the XRD experimental result. Although this study implies much stricter process conditions for diamond growth by ion beam deposition compared with other methods, it demonstrates the attainability of this diamond deposition by controlling a favourable dynamic process. We believe that this work could lead to a better understanding of the nature of the ion–diamond interaction and the application of the ion beam technique.

Acknowledgments

One of the authors (Zhu) is grateful to the Project sponsored by SRF for ROCS, SEM, the Natural Science Foundation of Anhui province (No 03044702), and the National Natural Science Foundation (No 19835030) of the People's Republic of China.

References

[1] Yoshimoto M, Yoshida K, Maruta H, Hishitani Y, Koinuma H, Nishio S, Kakihana M and Tachibana T 1999 *Nature* **399** 340
[2] Grossman E, Lempert G D, Kulik J, Marton D, Rabalais J W and Lifshitz Y 1996 *Appl. Phys. Lett.* **68** 1214
[3] Saito S and Oshiyama A 1991 *Phys. Rev. Lett.* **66** 2637
[4] Regueiro M N, Monceau P and Hodeau J L 1992 *Nature* **355** 237
[5] Zhu X D, Xu Y, Naramoto H, Narumi K and Miyashita K 2002 *J. Phys.: Condens. Matter* **14** 5083
[6] Bundy F P and Kasper J S 1967 *J. Chem. Phys.* **46** 3437
[7] Yagi T, Utsumi W, Yamakata M, Kikegawa T and Shimomura O 1992 *Phys. Rev.* B **46** 6031
[8] Wu B R and Xu J 1998 *Phys. Rev.* B **57** 13355
[9] Knight D S and White W B 1989 *J. Mater. Res.* **4** 385
[10] Maruyama K, Makin M, Kikukawa N and Shiraishi M 1992 *J. Mater. Sci. Lett.* **11** 116
[11] Yarbrough W A and Messier R 1990 *Science* **247** 688
[12] Sharda T, Umeno M, Soga T and Jimbo T 2000 *Appl. Phys. Lett.* **77** 4304
[13] Cuo Y P, Lam K L, Lui K M, Kwok R W M and Hui K C 1998 *J. Mater. Res.* **13** 2315
[14] Sun X S, Wang N, Zhang W J, Woo H K, Han X D, Bello I, Lee C S and Lee S T 1999 *J. Mater. Res.* **14** 3204

[15] Christian J F, Wan Z and Anderson S L 1993 *J. Chem. Phys.* **99** 3468
[16] Beck R D, Rockenberger J, Weis P and Kappes M M 1996 *J. Chem. Phys.* **104** 3638
[17] Hvelpund P, Andersen L H, Haugen H K, Lindhard J, Lorents D C, Malhotra R and Ruoff R 1992 *Phys. Rev. Lett.* **69** 1915
Foltin M, Lezius M, Scheier P and Mark T D 1993 *J. Chem. Phys.* **98** 9624
[18] Gruen D M, Liu S, Krauss A R, Luo J and Pan X 1994 *Appl. Phys. Lett.* **64** 1502
[19] Zhou D, McCauley T G, Qin L C, Krauss A R and Gruen D M 1998 *J. Appl. Phys.* **83** 540
[20] Zhou D, Gruen D M, Qin L C, McCauley T G and Krauss A R 1998 *J. Appl. Phys.* **84** 1981
[21] Marks N A 1997 *Phys. Rev.* B **56** 2441
[22] Banhart F and Ajayan P M 1996 *Nature* **382** 433
[23] Zaiser M and Banhart F 1997 *Phys. Rev. Lett.* **79** 3680